PURDUE UNIVERSITY
SCHOOL OF AERONAUTICS AND ASTRONAUTICS

(NASA-CR-175366) THREE-DIMENSIONAL MEASUREMENTS OF FATIGUE CRACK CLOSURE Semiannual Status Report (Purdue Univ.) 19 p HC A02/MF A01

N84-17616

Unclas
G3/39 18276

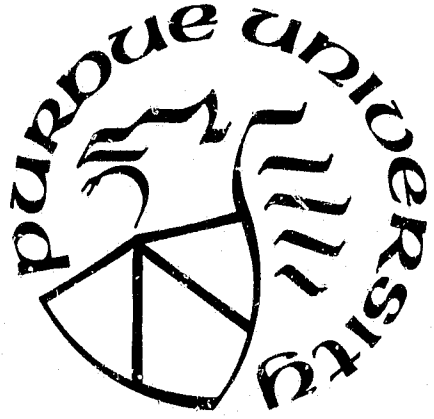

West Lafayette, Indiana 47907

Three-Dimensional Measurements of Fatigue Crack Closure

Semiannual Status Report

for

NASA Grant No. NAG-1-321

submitted

by

A.F. Grandt, Jr.

School of Aeronautics and Astronautics

Grissom Hall

Purdue University

West Lafayette, Indiana 47907

February 1984

OBJECTIVE

The objective of this effort is to determine three-dimensional fatigue crack opening profiles in transparent polymer test specimens. The load required to separate crack faces will be measured along the crack profile at various positions through the specimen thickness. A particular goal is to compare crack opening loads at the specimen surface (under plane stress conditions) with measurements made under plane strain conditions in the specimen interior. The fatigue crack opening load will be correlated with fatigue crack retardation behavior caused by peak overloads, and the results will be discussed in terms of three-dimensional aspects of the fatigue crack closure mechanism for fatigue crack retardation.

PROGRESS

The current grant was awarded January 27, 1983 for a period of 12 months. A no-cost time extension running through June 30, 1984 was approved on September 12, 1983. This section summarizes progress toward the grant goals from August 1983 through January 1984. During this period, several fatigue crack growth/overload experiments have been conducted with polycarbonate test specimens, and an optical interference technique has been successfully used to measure crack surface displacements. This data is currently being analyzed in the context of three-dimensional aspects of fatigue crack closure. Some typical results are described in the remainder of this report.

The test specimens consist of 1.5 x 0.8 x 7.0 in. edge-cracked beams which are loaded in four-point bending at a cyclic frequency of 4 Hz. All specimens are machined from the same sheet of polycarbonate (a transparent polymer) and are annealed prior to testing to relieve possible residual stresses. As discussed in the previous progress report, fatigue cracks are

initiated and grown at relatively low stress intensity factor levels ($\Delta K < 300$ psi-in$^{1/2}$) in order to get the smooth crack surfaces required for the optical interference experiments. Since the specimens are optically transparent, the crack plane is readily observed and photographed during the fatigue testing. These photographs are then measured to determine the crack dimensions as a function of elapsed cycles.

After initiation, the cracks are grown at constant cyclic K levels to obtain a linear crack length versus cycles response. Following establishment of steady state crack growth, single peak overloads are applied, and testing is resumed at the original baseline K level. The crack retardation period is readily observed on the resulting crack growth curves.

Figures 1 through 4 present typical fatigue crack growth results for two tests. Figure 1 gives the average through-the-thickness crack length for a specimen cycled at a baseline stress intensity of 300 psi-in$^{1/2}$. The resulting delay caused by a single peak overload of 1200psi-in$^{1/2}$ is readily apparent on this figure. Figure 2 compares the crack length measured on the specimen side with that measured in the middle for this particular specimen. Note that, as expected, the crack grows faster in the specimen interior than at the free surface. Figures 3 and 4 present similar data for a specimen cycled at a baseline K of 270 psi-in$^{1/2}$ and subjected to an overload of 1350 psi-in$^{1/2}$ (overload factor of 5). Figure 3 presents the average crack length as a function of elapsed cycles, while Fig. 4 compares the surface crack length dimension with that measured in the specimen interior. Note in Fig. 4 that the surface dimension is retarded more than the mid-thickness crack length (note scale change). This behavior is expected due to the difference between the plane stress plastic zone at the free surface and plane strain yielding in the specimen interior.

The main objective of the current research is to determine the three-dimensional crack surface opening behavior before and after application of tensile overloads. In particular, it is desired to compare the free surface and mid-thickness crack closure loads during the course of the fatigue cycling. The selection of the transparent polymer test material allows use of optical interferometry to measure the crack surface separation as a function of applied load.

The physics involved in the interference mechanism are discussed in the grant proposal. For present purposes, let it simply be stated that when the cracked specimen is viewed with a monochromatic light source (a sodium vapor lamp is used here), optical interference patterns are created in the crack plane. These fringes are proportional to the crack surface separation and are readily photographed as a function of applied load. Measurement of the fringe photographs (a projector/digitizing) table apparatus is used here) allows one to determine the crack opening profiles. Since the fringe patterns contain complete three-dimensional crack surface displacement data, crack opening in the specimen interior can be measured and compared with that observed on the specimen surface.

Typical fatigue crack opening profiles determined from the interference fringe patterns are given in Figs. 5 to 8 for specimen 1. Here the crack surface displacement (measured in fringe units) is plotted versus distance from the crack tip for various applied load levels. Figure 5 gives the crack surface opening measured on the specimen surface (plane stress conditions) while Fig. 6 gives the plane strain profiles determined at mid thickness. In both cases, the crack profiles are determined after a period of steady state cycling at $\Delta K = 300$ psi-in$^{1/2}$. Note in Fig. 5 that the crack tip is held shut for a significant period of initial loading, while the closure load is much

less in the specimen interior as shown in Fig. 6. Figures 7 and 8 present the surface and interior crack opening profiles immediately following application of the 1200 psi-in$^{1/2}$ overload. Additional profiles were obtained later in the test following recovery from the overload.

Figure 9 summarizes the crack surface separation load as measured at various points through the specimen thickness for specimen 1. Here the stress intensity level required to cause crack tip separation (divided by the baseline K level of 300 psi-in$^{1/2}$) is plotted versus the dimensionless distance from the specimen surface. The free surface values (normalized distance = 0.0) are obtained from Figs. 5 and 7, while the midplane opening loads (normalized distance = 0.5) come from Figs. 6 and 8. The remaining data are from additional analysis of the original fringe patterns. Note in Fig. 9 that the crack opening load decreased following application of the overload. The opening load was reduced to zero at the specimen interior, as crack tip blunting appears to permanently prop the crack tip opening. Although there still was free surface crack closure following the overload, the opening load was reduced. Figure. 10 presents similar results for specimen 2, which was cycled at a baseline K = 270 psi-in$^{1/2}$, with a 1350 psi-in$^{1/2}$ overload.

Figure 11 was prepared to to compare the crack opening profiles determined by the interference method with results obtained by conventional crack closure measurement methods. Here, the crack surface separation at a point 0.06 in. behind the crack tip is plotted as a function of applied load. The stress intensity level required to give an elastic force/displacement relation is shown as the point labeled "elastic Kopen." These data were obtained from the free surface crack opening profiles of specimen 1 prior to application of the overload (Fig. 5). Table 1 summarizes the crack opening load obtained in this manner for Specimen 1. Note that the opening load measured at various

distances behind the crack tip is given for the steady state condition, and for the first, tenth, and 1000th cycle following the overload. Results are given for measurements made at the free surface and in the specimen interior. These data indicate that the opening load (when defined as the force which yields elastic behavior) is increased at the specimen interior following application of the overload, and would tend to decrease crack growth rates in agreement with the closure mechanism for fatigue crack retardation.

Future work will be directed at obtaining additional experimental results. Particular emphasis will be given toward determining the relation between the crack tip blunting behavior which is observed from the crack opening profiles with the closure loads measured from the elastic load/displacement records. Conventional crack closure measurements will also be made with crack opening displacement gages and with strain gages bonded across the crack tip in order to compare those methods with the optical interference technique. Stress-strain curves will be obtained for the polycarbonate test material.

DIST(in) from tip	S-S Kopen,e middle	S–S Kopen,e surface	1st cycle AO middle	1st cycle AO surface	10th cycle AO middle	10th cycle AO surface	10^3 cycles AO middle	10^3 cycles AO surface
.0075	36	74	60	—	67	76	60	—
.0150	33	68	59	63	62	74	59	67
.0300	33	65	59	62	62	68	59	65
.0600	33	60	59	62	62	68	59	64
.0900	—	58	—	60	—	68	—	63
.1200	—	58	—	60	—	68	—	62

Table 1. A summary of elastic K_{open} values for different conditions in the experiment.(unit of Psi-sqrt in)

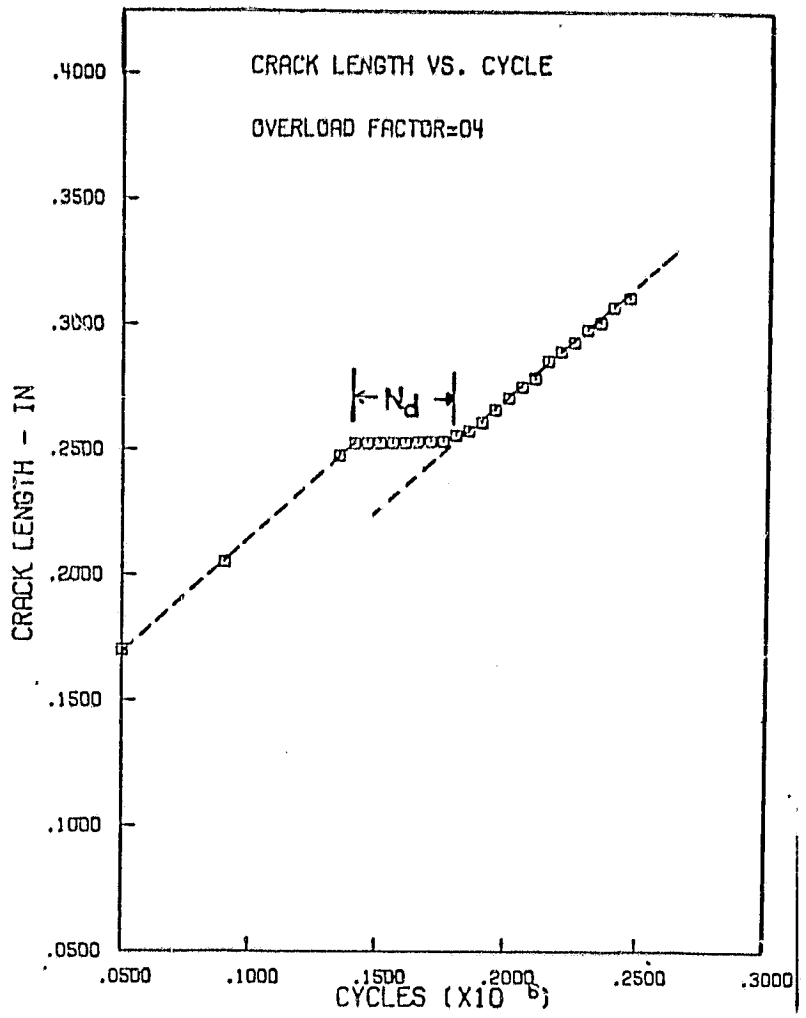

Figure 1 Average through-the-thickness fatigue crack length versus cycles curve for Specimen 1 (ΔK = 300 psi-in$^{1/2}$, single peak overload = 1200 psi-in$^{1/2}$).

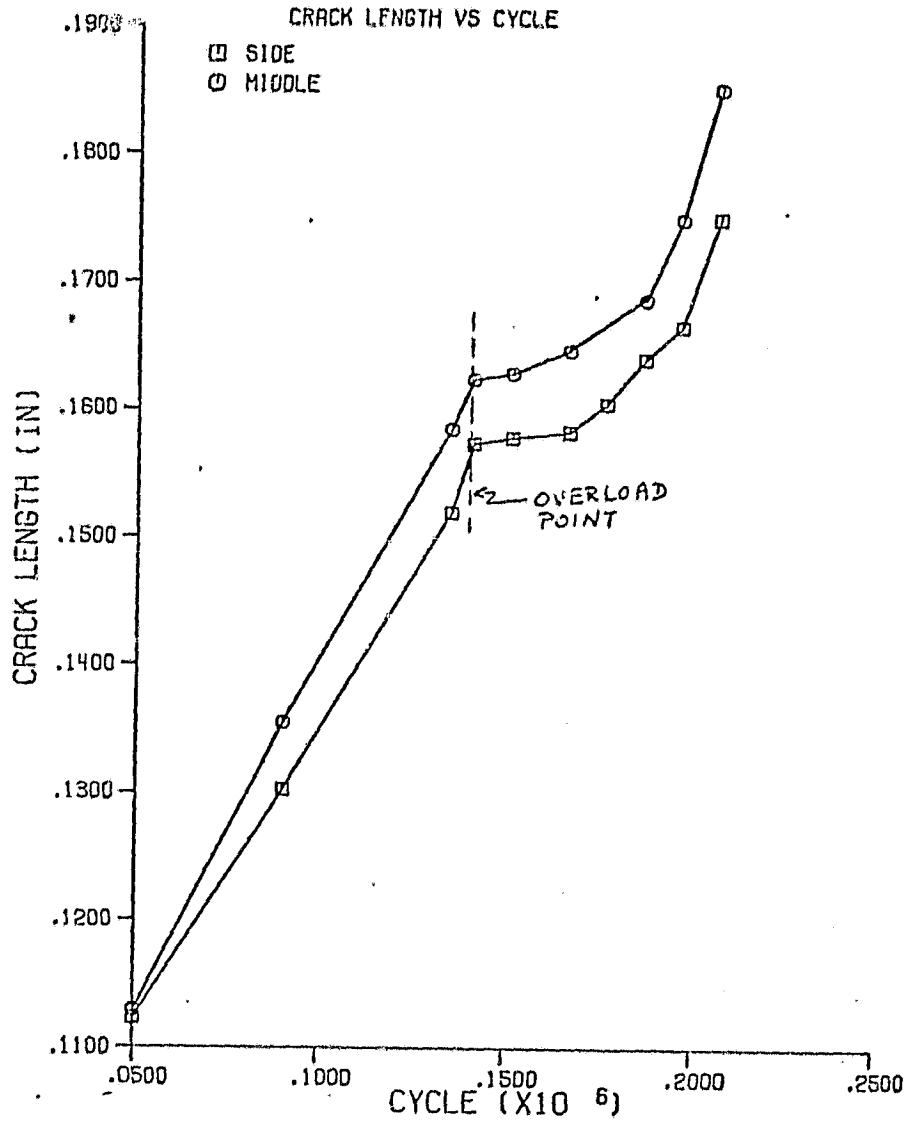

Figure 2 Comparison of the cyclic growth of crack dimension measured at the side and middle of specimen 1 (ΔK = 300 psi-in$^{1/2}$, overload = 1200 psi-in$^{1/2}$).

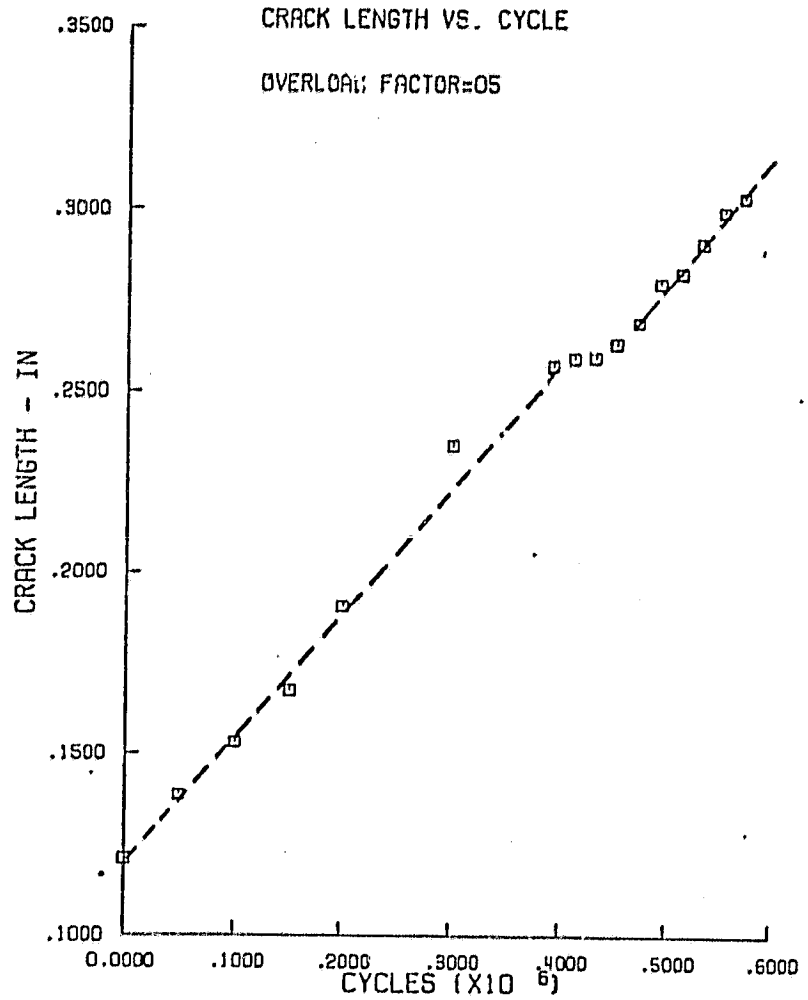

Figure 3 Average through-the-thickness fatigue crack growth for specimen 2 (ΔK = 270 psi-in$^{1/2}$, peak overload = 1350 psi-in$^{1/2}$).

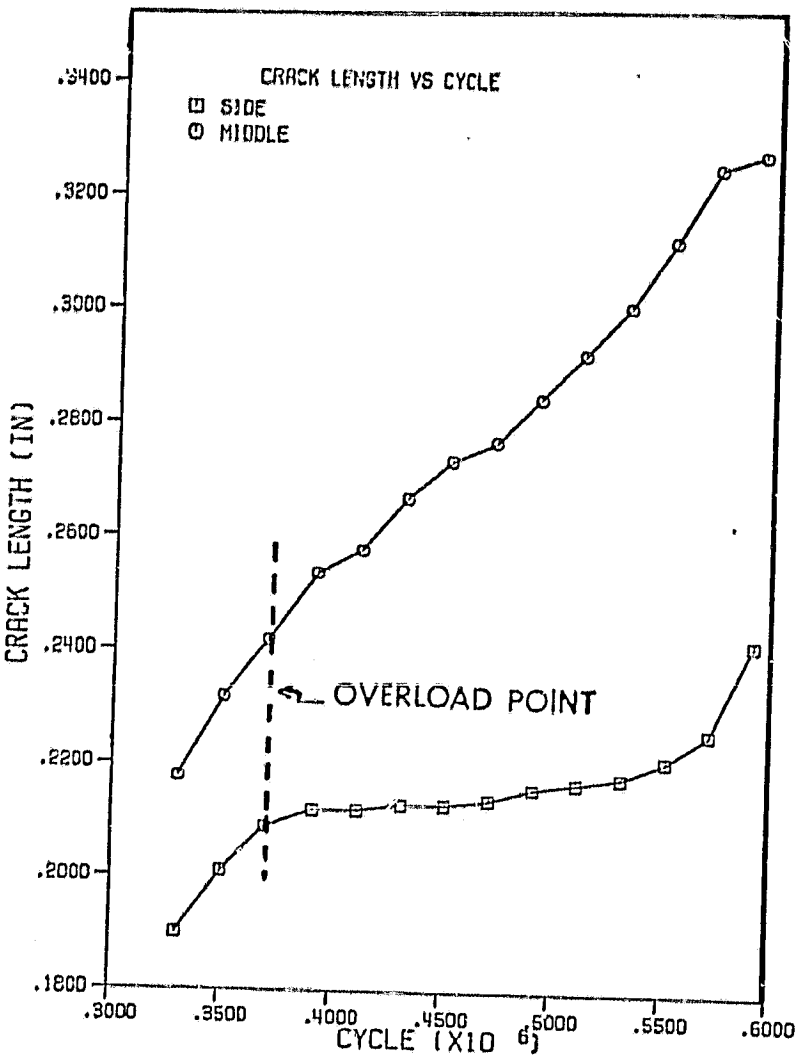

Figure 4 Comparison of cyclic growth of surface (side) and interior (middle) crack dimensions for specimen 2 (ΔK = 270 psi-in$^{1/2}$, overload = 1350 psi-in$^{1/2}$).

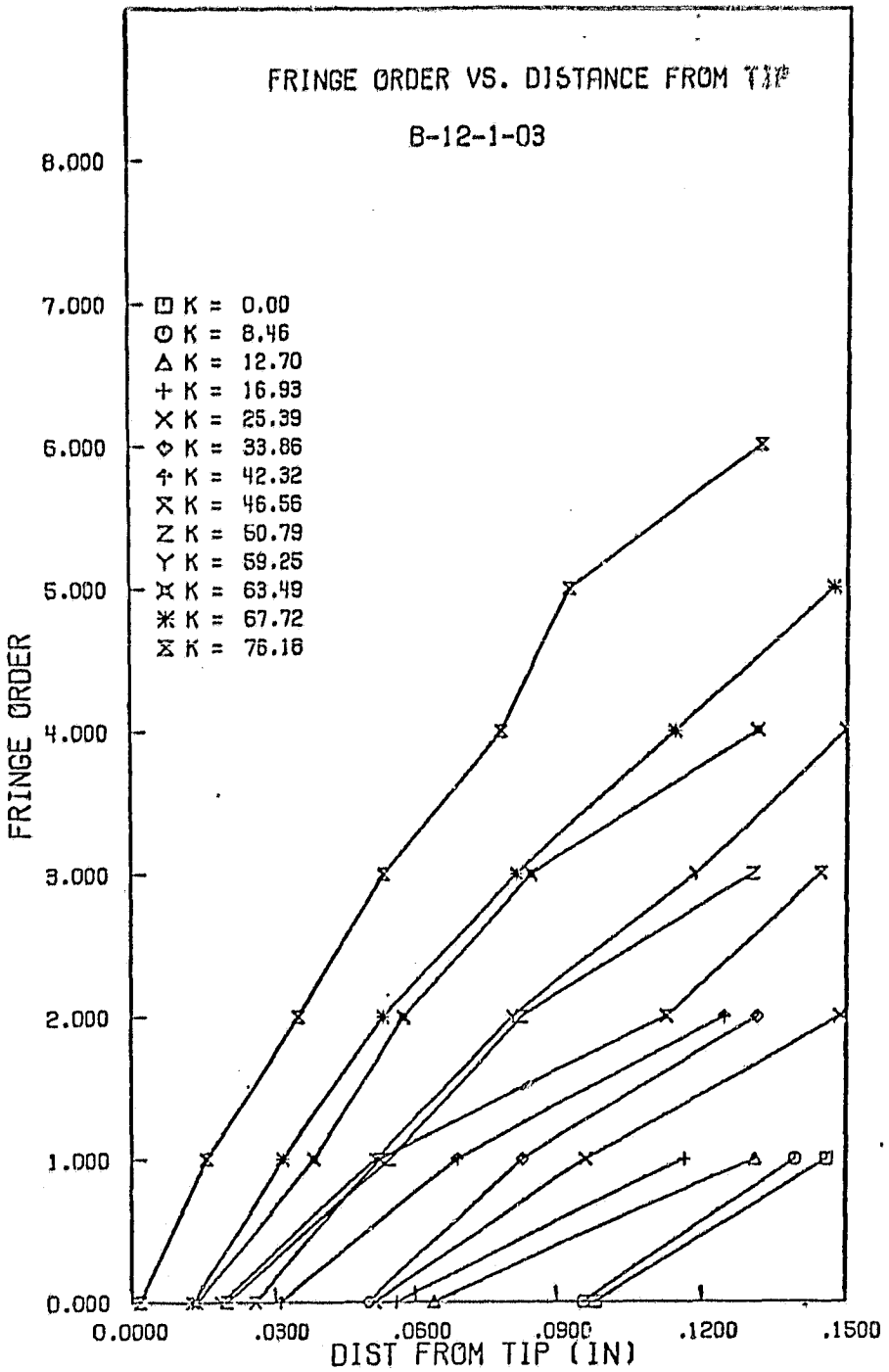

Figure 5 Free surface crack opening profiles as a function of applied load for Specimen 1 (steady state condition).

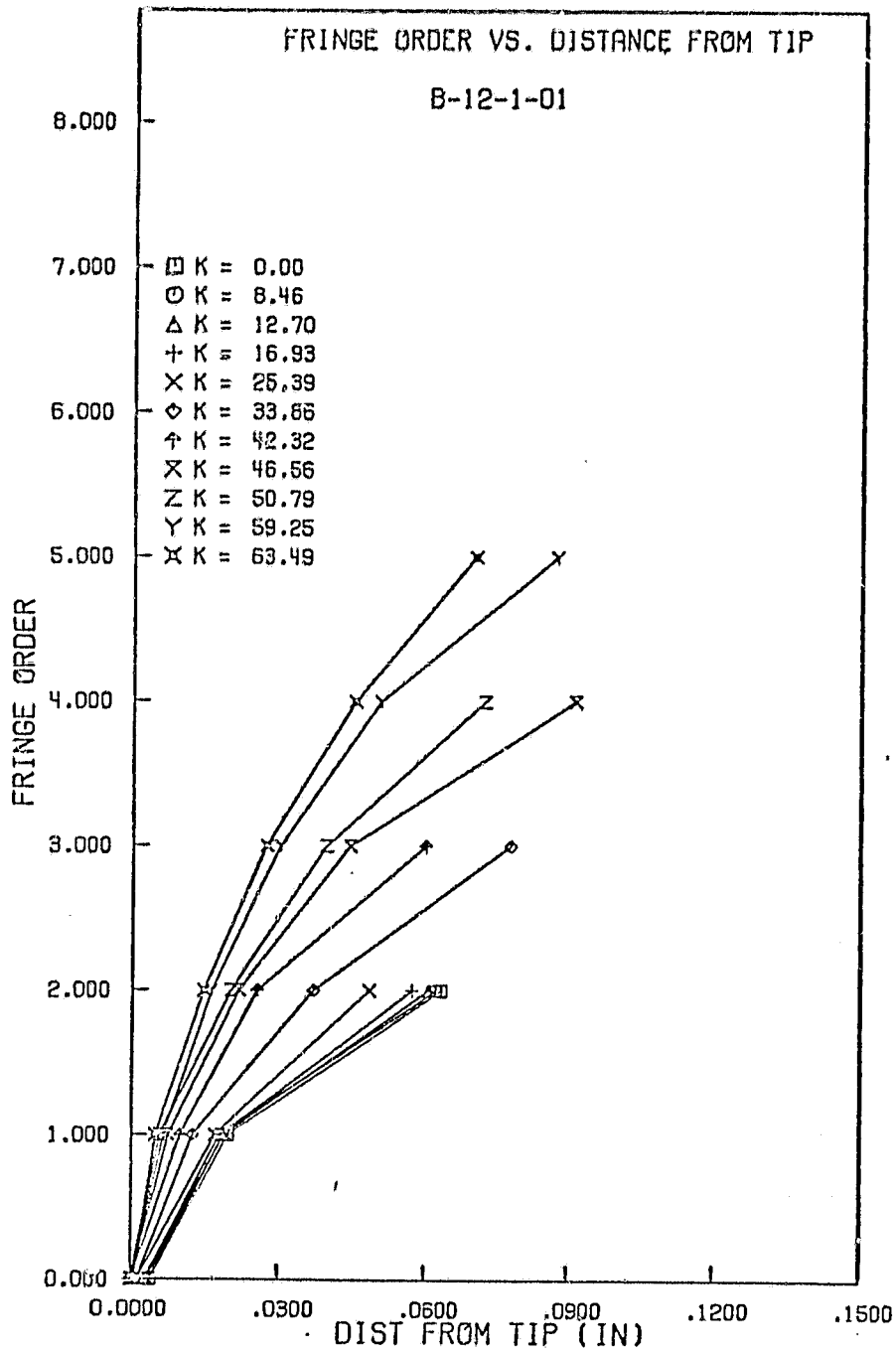

Figure 6 Midplane crack opening profiles as a function of applied load for Specimen 1 (steady state conditions).

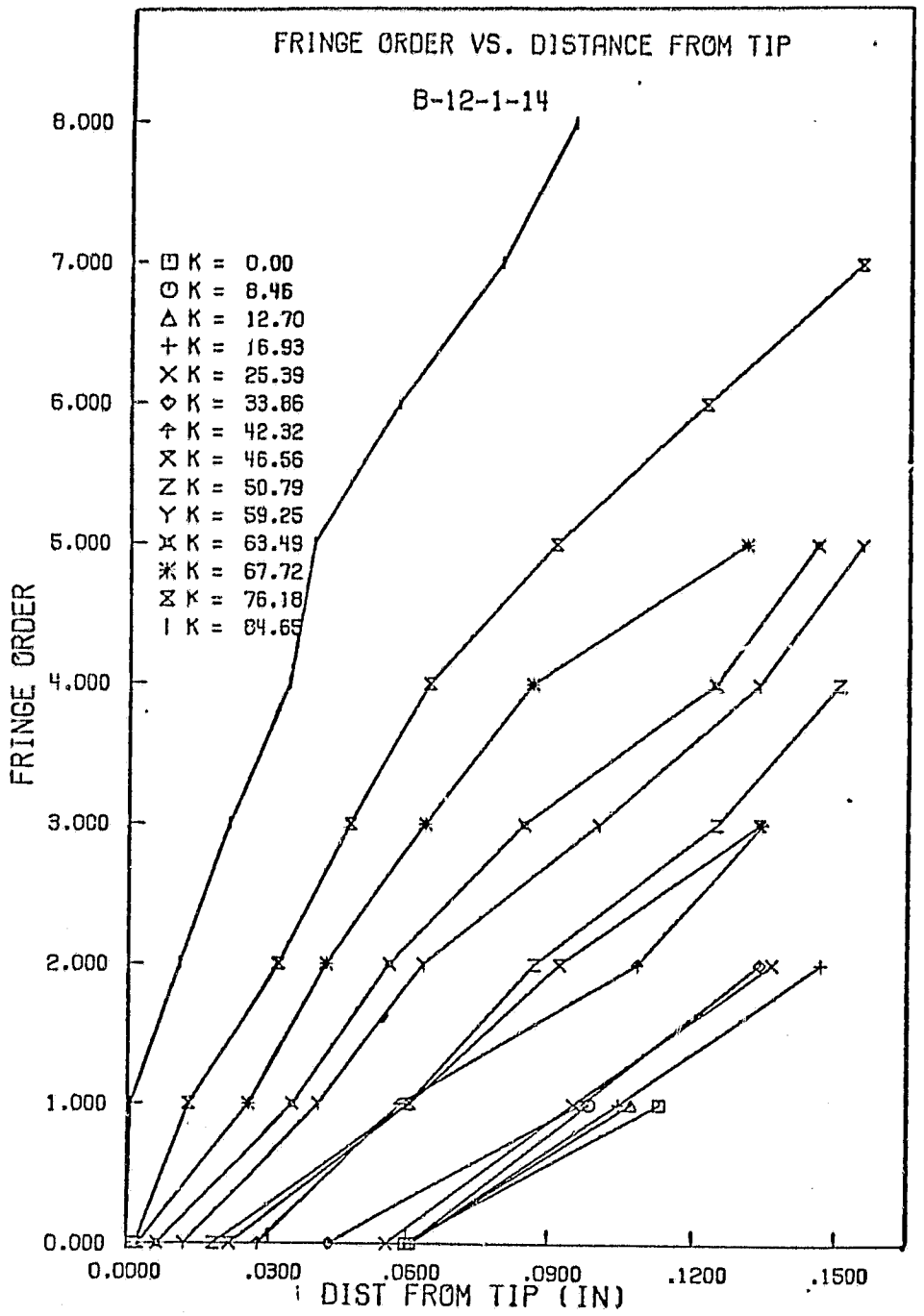

Figure 7 Free surface crack opening profiles for first cycle following overload (specimen 1).

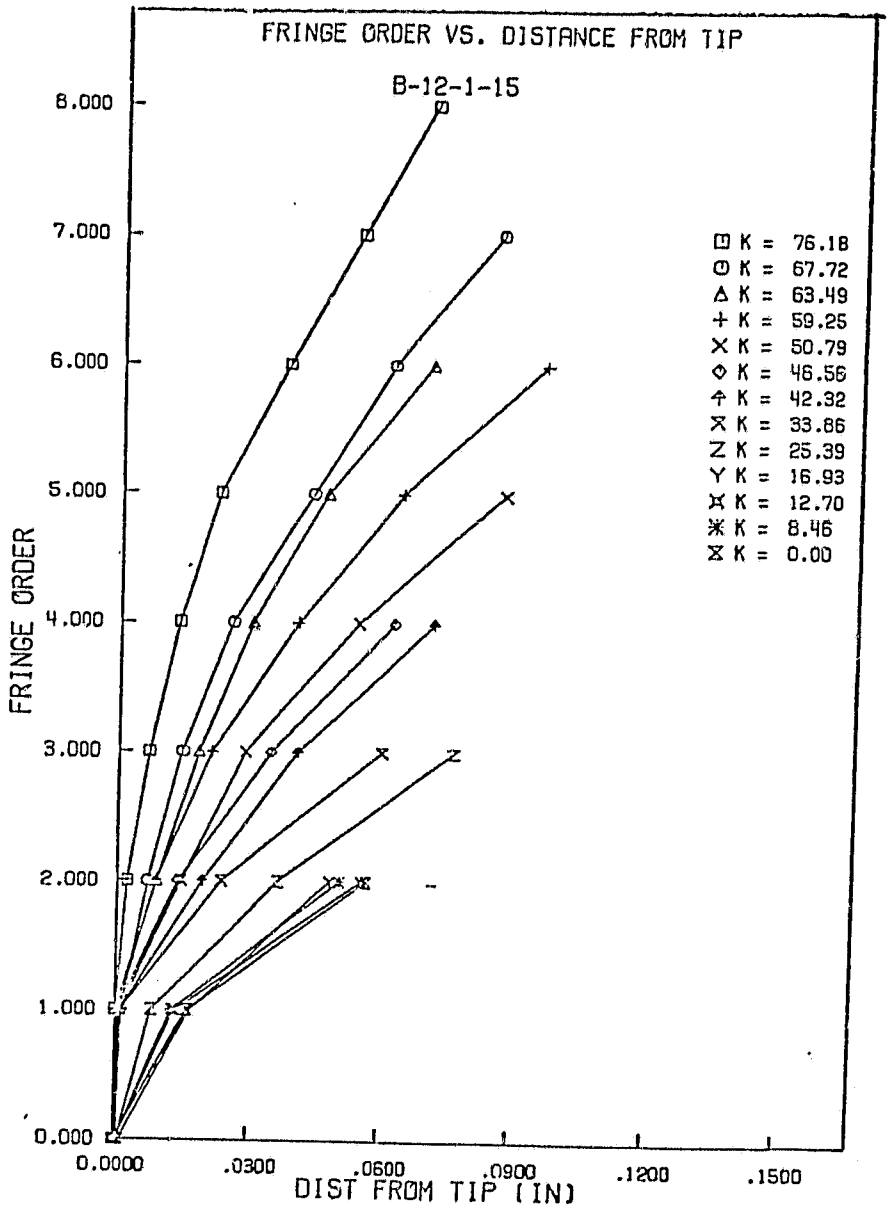

Figure 8 Midplane crack opening profiles for first cycle after overload (specimen 1).

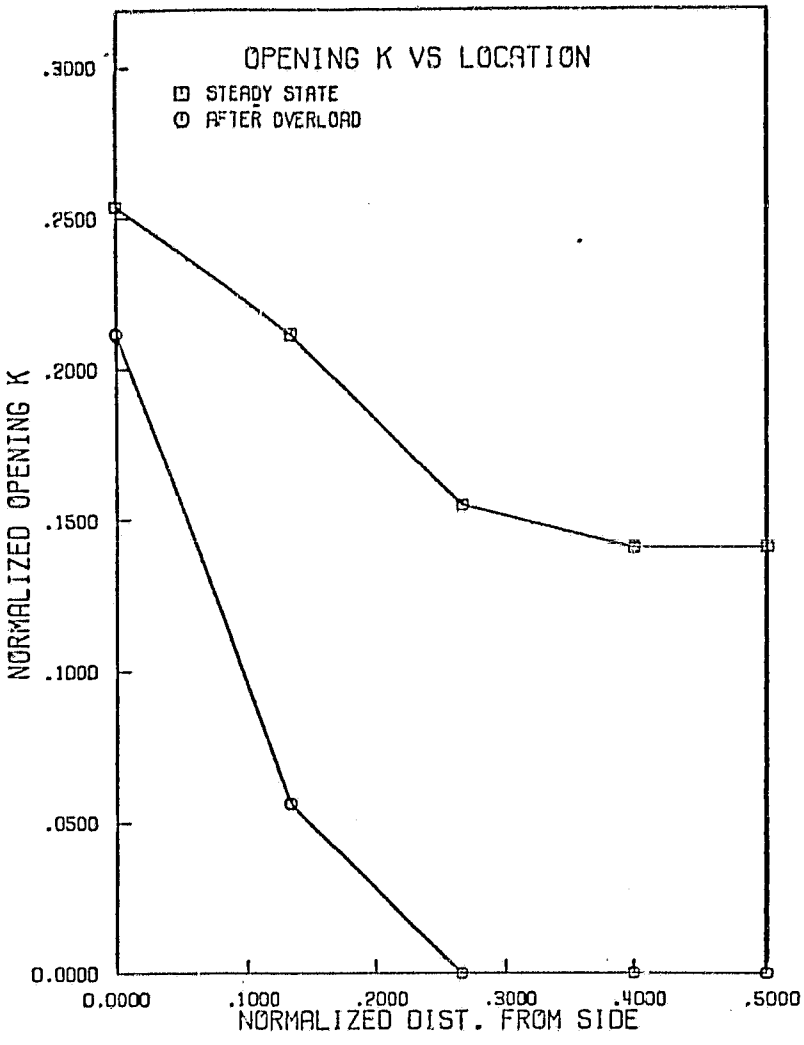

Figure 9 Comparison of dimensionless crack opening load measured at various points though the specimen thickness before and after application of overload (specimen 1, cyclic $K = 300$ psi-in$^{1/2}$, overload = 1200 psi-in$^{1/2}$).

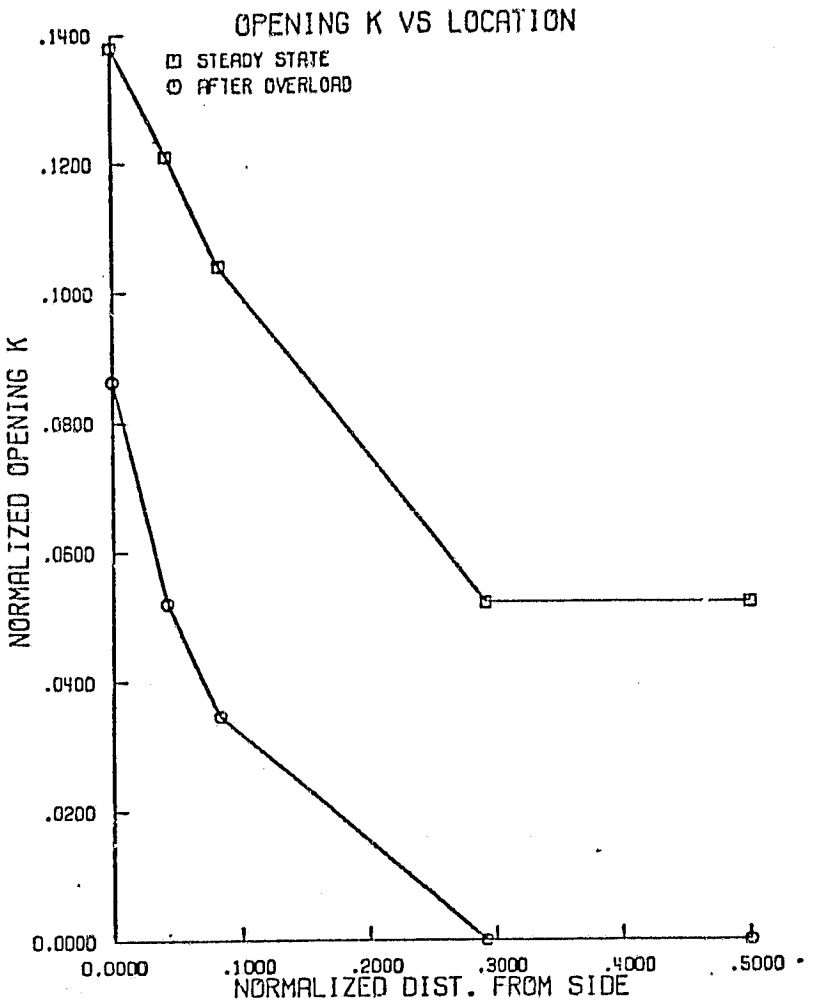

Figure 10 Comparison of dimensionless crack opening load measured at various points through the specimen thickness before and after overload (specimen 2, cyclic K = 270 psi-in$^{1/2}$, overload = 1350 psi-in$^{1/2}$).

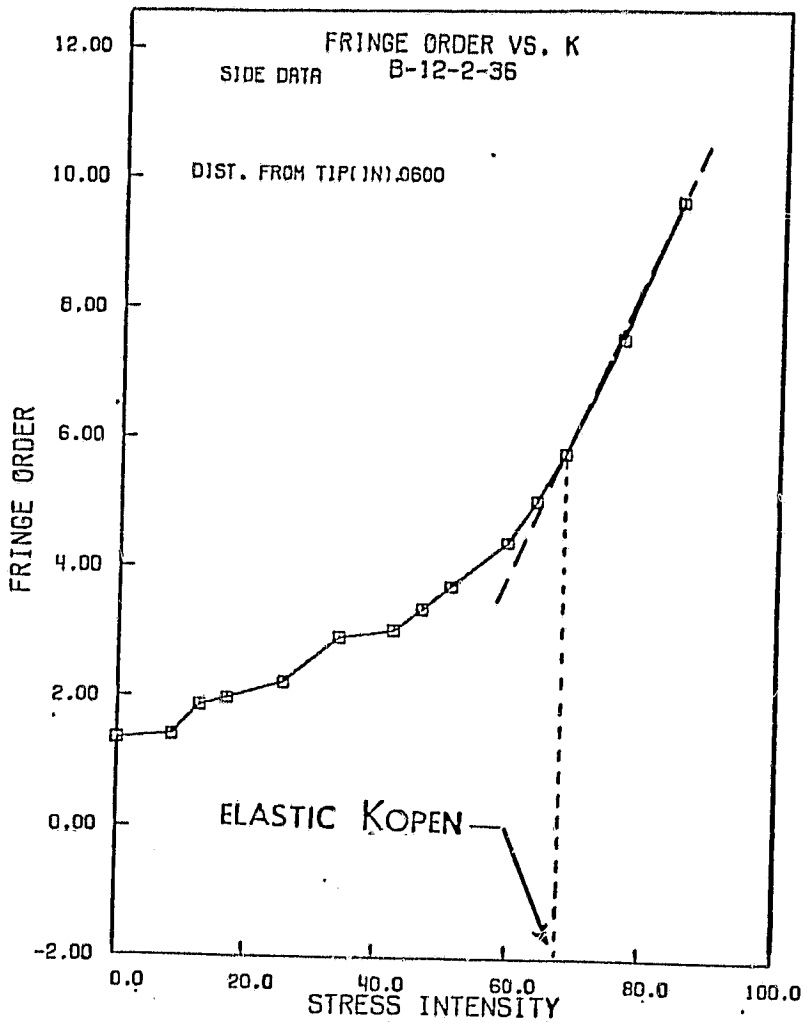

Figure 11 Crack tip separation measured on specimen surface at a distance of 0.06 in, behind crack tip.